Electrocatalysis (2015) 6:127–131
DOI 10.1007/s12678-015-0246-1

LETTER

A *DEMS* Study of the Reduction of CO_2, CO, and HCHO Pre-Adsorbed on Cu Electrodes: Empirical Inferences on the CO_2RR Mechanism

Alnald Javier · Brian Chmielowiec · Jean Sanabria-Chinchilla · Youn-Geun Kim · Jack H. Baricuatro · Manuel P. Soriaga

Published online: 27 January 2015

Introduction

The effective abatement of atmospheric carbon through its conversion via electrochemical reduction to pure and oxygenated hydrocarbon fuels relies on the ability to control product selectivity at viable current densities and faradaic efficiencies. One critical aspect is the choice of the electrode and, in the CO_2-reduction electrocatalyst landscape, copper sits as the only metal known to deliver a remarkable variety of reduction products other than carbon monoxide and formic acid [1–7]. However, much better catalyst performance is needed. The overall energy efficiency of copper is less than 40 % [1–4], and its nominal overvoltage at benchmark current densities remains unacceptably large at ca. 1 V. The diversity of the product distribution also becomes a major inconvenience in the likelihood that only one product is desired; unless, of course, if the selectivity window for such product is already known. Several experimental parameters influence the product selectivity of the CO_2 reduction reactions (hereafter referred to as CO_2RR); the more obvious include the composition and the crystal structure of the catalyst surface [1, 5, 6, 8], the applied potential [1–6], the solution pH [1, 9], and the supporting electrolyte [1]. The documentation, at the atomic level, of the mechanistic origins of the CO_2RR selectivity of copper demands a systematic combination of ex situ, in situ, and *operando* techniques to interrogate the electrode surface, pristine and modified, prior to, during, and after the reduction reaction; the task includes not only the analysis of reaction-product distributions but also the identification of surface intermediates that serve as the precursor states for each reaction pathway.

We recently studied the nature of well-defined Cu(*hkl*) single-crystal surfaces that, similar to "real-world" catalysts, were handled in air. Such investigation is pertinent since Cu is a well-known scavenger of molecular oxygen; hence, CO_2RR electrocatalysis must first contend with the initial presence of multilayers of disordered copper oxides [10]. It was found that the oxides are actually easily reduced electrochemically back to the metal; in addition, even if the oxided single-crystal surface is severely disordered, cathodic reduction completely regenerates the original ordered structure [11]. Most recently, we discovered that a polycrystalline Cu electrode held at a fixed negative potential in the CO_2RR region in KOH, undergoes stepwise surface reconstruction, first to Cu(111) and then to Cu(100) [12]. The results help explain the Cu(100)-like behavior of Cu(pc) in terms of CO_2RR product selectivity [5, 13].

In the work described in this *Letter*, we have applied differential electrochemical mass spectrometry (DEMS) of *pre-adsorbed* reactants and intermediates as a complementary experimental approach in the study of the mechanistic pathways for the Cu-catalyzed CO_2 reduction reactions; the reactant was CO_2 and the intermediates were CO and HCHO. The reduction products monitored by mass spectrometry were H_2, CO (from CO_2), CH_4, $H_2C{=}CH_2$ and CH_3CH_2OH.

Experimental

The principles of DEMS and its applications to electrochemical surface science have been amply discussed and reviewed

A. Javier · B. Chmielowiec · J. Sanabria-Chinchilla · Y.-G. Kim · J. H. Baricuatro · M. P. Soriaga
Division of Chemistry and Chemical Engineering, Joint Center for Artificial Photosynthesis, California Institute of Technology, Pasadena, CA 91125, USA

M. P. Soriaga (✉)
Department of Chemistry, Texas A&M University, College Station, TX 77843, USA
e-mail: msoriaga@caltech.edu

[14, 15]; a stand-alone DEMS system, not integrated with an ultrahigh-vacuum-electrochemistry apparatus [16, 17], was deemed sufficient for this study since it does not involve well-defined single-crystal Cu electrodes. An HPR-20 quadrupole mass spectrometer (Hiden Analytical, Warrington, England) was utilized with only minor modifications in conjunction with a custom-crafted DEMS cell; in operation, the scanning electron multiplier detector voltage was set at 950 V, the emission current at 50 μA. A three-electrode DEMS cell, similar to what was used in previous studies [18], was fabricated from polyether ether ketone. The working electrode was a disk-shaped 99.99 %-pure Cu foil (Goodfellow, Coraopolis, PA), with solution-exposed geometric surface area of 0.90 cm^2; Ag/AgCl (1 M KCl) was the reference electrode (CH Instruments, Austin, TX), and a Pt wire (Goodfellow, Coraopolis, PA) served as the counter electrode. A 20-μm-thick Teflon membrane with 20-nm porosity was located between the thin-layer cell and the mass spectrometer port; only volatile, especially if hydrophobic, products are able to pass through the membrane. A cylindrical glass spacer, ca. 50 μm in thickness, situated between the Cu electrode and the plastic membrane, limited the volume of liquid inside the thin-layer electrolytic cell to less than 10 μL. The cell was operated without forced convection; spent sample solutions were expelled and replenished between experimental trials. A porous glass frit was inserted between the working cathode and counter anode to prevent ingress and re-oxidation of the CO_2RR products at the anode.

Prior to each experiment, the Cu disk was metallographically polished and then electrochemically annealed in 85 % phosphoric acid, rated with less than 0.01 % trace metals (Sigma-Aldrich, St. Louis, MO), at 2.1 V for 180 s; a 99.8 % pure graphite rod (Alfa Aesar, Ward Hill, MA) was used as counter electrode. The Cu electrode surface thusly treated had not been shielded from air and, hence, contained CuO and Cu_2O [11]. Prior to introduction of the sample compounds in the DEMS cell, the Cu electrode was held at a negative potential for 180 s to remove all vestiges of surface oxides [10, 11]. The 0.1 M $KHCO_3$ solutions of CO_2 and CO were prepared separately by a purge with high-purity gases at a partial pressure of 1 atm; based on Henry's law [19], the equilibrium concentrations were 35 mM for CO_2 and 1.0 mM for CO. A 20 mM solution of HCHO was prepared from a commercial methanol-free reagent (Thermo Scientific, Rockford, IL). The pH of the bicarbonate solutions was initially at 8.2; however, after the CO_2 purge, the pH for the CO_2 solution dropped to 6.8. Control (blank) trials were carried out under identical conditions except that the solution, purged with high-purity N_2 gas, did not contain any of the subject compounds.

Electrochemistry experiments were conducted with a Bio-Logic SP-300 potentiostat (BioLogic Science Instruments, Claix, France) equipped for electrochemical impedance spectroscopy (EIS). Potentiostatic EIS measurements were performed at 100 kHz to determine the uncompensated solution resistance (R_u); 85 % of R_u was electronically compensated. Linear-sweep current-potential plots were obtained at a scan rate of 1 mV/s.

Results and Discussion

Strictly, the subject compounds should not be expected to adsorb on copper under CO_2RR conditions because, on clean Cu in ultrahigh vacuum, all three species desorb at temperatures below −100 °C [20, 21]. Their heats of adsorption are rather low: ca. 6 kcal mol^{-1} for both CO_2 and HCHO [21, 22] and 12 kcal mol^{-1} for CO [20]. How the adsorption enthalpies are influenced by the presence of solvent molecules and supporting electrolyte ions in the compact layer at highly negative potentials is not known; it is logical to surmise, however, that the extent of adsorption would be diminished simply because of heightened competition from electroadsorbates on the negatively charged surface.

The term *pre-adsorption* is legitimized by the certainties that: (i) Only one compound at a time is introduced into the thin-layer electrochemical cell prior to electrolysis. (ii) The copper electrode is pre-exposed to neither the other reactants nor the reduction products. The sole adsorption equilibrium that exists is between the compound in solution and on the surface. (iii) The reduction reactions are both electrocatalytic and heterogeneous. Adsorption is a pre-requisite to the electron transfer processes. (iv) The cell is stationary and not flow-through; perturbation of the adsorption equilibrium arises only from the electron transfer reactions and not by exogenous factors such as forced convection. An added benefit is that the solution thickness is smaller than the Nernst diffusion layer; if desired, exhaustive potentiostatic electrolysis can be accomplished in little time.

Figure 1 shows the voltammetric plots for the electrochemical reduction of CO_2, CO, and HCHO adsorbed on Cu. There are only minimal differences between the three plots because, as it is well known, the features for the CO_2/CO/HCHO cathodic reactions are masked by the sizable contribution of the hydrogen evolution. In fact, were it not for the slight but discernible dip in the hydrogen current-potential curve, the three plots would be indistinguishable from that of a blank solution. The slight drop has been attributed to the poisoning of the Cu surface by adsorbed CO [1, 5]. Such interpretation, however, is not borne out by the present result for HCHO, an adsorbate more feeble than CO; it shows the same current dip even in the absence of carbon monoxide. Since the adsorption strength of hydrogen is at least four times larger than that of CO [23], it is

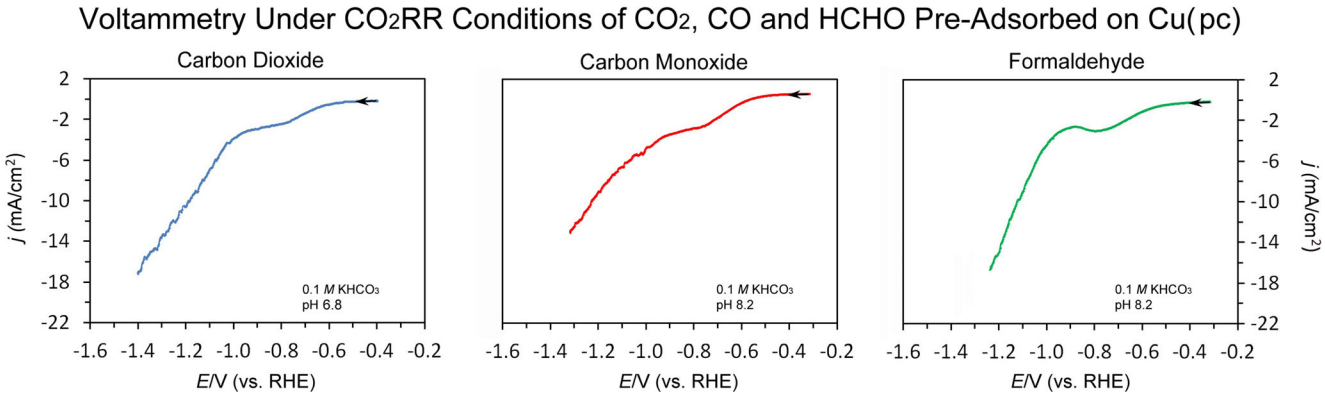

Fig. 1 Voltammetric plots of a metallographically polished polycrystalline copper electrode in aqueous 0.1 M $KHCO_3$ in the presence of CO_2, partial pressure $P°=1$ atm and, from Henry's law, solution concentration $C°=35$ mM; CO, $P°=1$ atm, and $C°=1.0$ mM; HCHO, $C°=20$ mM. Potential sweep rate=1.0 mV s−1. Temperature=25 °C

unclear how the weakly adsorbed CO can impede the chemisorption of the much more strongly bound hydrogen.

Survey mass-spectrometric-current voltammograms (MSCV) for pre-adsorbed CO_2, CO, and HCHO showed that only H_2, CO, CH_4, $H_2C{=}CH_2$, and CH_3CH_2OH were detectable; control experiments yielded only hydrogen. Hence, only those compounds were monitored, although CO as a product was assayed only for the CO_2 sample. The results are compiled in Fig. 2. It is immediately obvious that the scatter in the MSCV data is substantial for the reduction of both CO_2 and CO, but non-existent for HCHO. The imprecision of the results is most likely because CO and CO_2 are water-insoluble gases whose solution concentrations are transiently perturbed by the concomitant evolution of hydrogen gas; the equilibrium concentration, however, is maintained by Henry's law, as the partial pressure of the gas above the solution was kept constant. HCHO, on the other hand, is exceedingly soluble in water, 400 g L^{-1}. For easier visual comparison of the MSCV results, the solid lines are provided in Fig. 2; the traces do not represent theoretical simulations but are mere sextic polynomial fits to generate trend lines.

Four features in Fig. 2 bear valuable empirical insights into the reaction mechanism of the CO_2RR on Cu electrodes. (i) The MSCV data for CO_2 and CO are virtually identical in all aspects with regard to the production of hydrogen, methane, ethylene, and ethanol. The similarity is not unexpected since it is now a widely held view that, upon CO_2 reduction on Cu, CO is the first product, as well as the first intermediate for further cathodic reactions. (ii) The MSCV plot for HCHO is drastically different from that of CO_2 or CO. The most obvious is the total absence of ethylene in the product distribution. It can thus be inferred that adsorbed HCHO is not a precursor for C=C *double-bond* formation. (iii) The data for HCHO, specifically its reduction-product distribution, indicates that it is also an intermediate in the synthesis of methane and ethanol. Evidently, the generation of CH_4 and CH_3CH_2OH from adsorbed CO occurs via two pathways: one involves a postulated surface species, protonated CO ($Cu–OCH^+$) that is formed in a rate-determining step [24, 25, 26], and the other relies on adsorbed HCHO, created after the slow CO-protonation step. (iv) The onset potential for the production of methane and ethanol from HCHO is ca. 300 mV less negative than that from CO. Clearly, this points to a substantially higher activation barrier for hydrocarbon conversions from CO than from HCHO, an implication not at variance with the theoretical prediction [24, 25, 26] just cited above. Explicitly stated, because the HCHO-to-CH_4 and HCHO-to-CH_3CH_2OH reactions transpire after the rate-limiting $Cu–OCH^+$-formation step, they cannot be as highly activated.

Summary

Differential electrochemical mass spectrometry (DEMS) of pre-adsorbed reactants (CO_2) and postulated intermediates (CO and HCHO) has been employed, for the first time, as a complementary approach in experimental mechanistic studies of the Cu-promoted electrochemical reduction of CO_2. Dilute solutions of CO_2, CO, and HCHO in aqueous $KHCO_3$ were placed separately in a DEMS stationary thin-layer electrochemical cell in contact with a polycrystalline Cu electrode and simultaneous faradaic-current and mass-spectrometric-current voltammograms were obtained for each of the solutions. The only reduction products detected by mass spectrometry were H_2, CH_4, $H_2C{=}CH_2$ and CH_3CH_2OH; CO was also assayed but only from the reduction of CO_2.

The results have prompted the following empirical inferences: (i) The slight but not imperceptible drop in the hydrogen evolution current may not be due to CO poisoning; it also exists for HCHO, an adsorbate more weakly bound than CO. In addition, the adsorption strength of H_2 is four

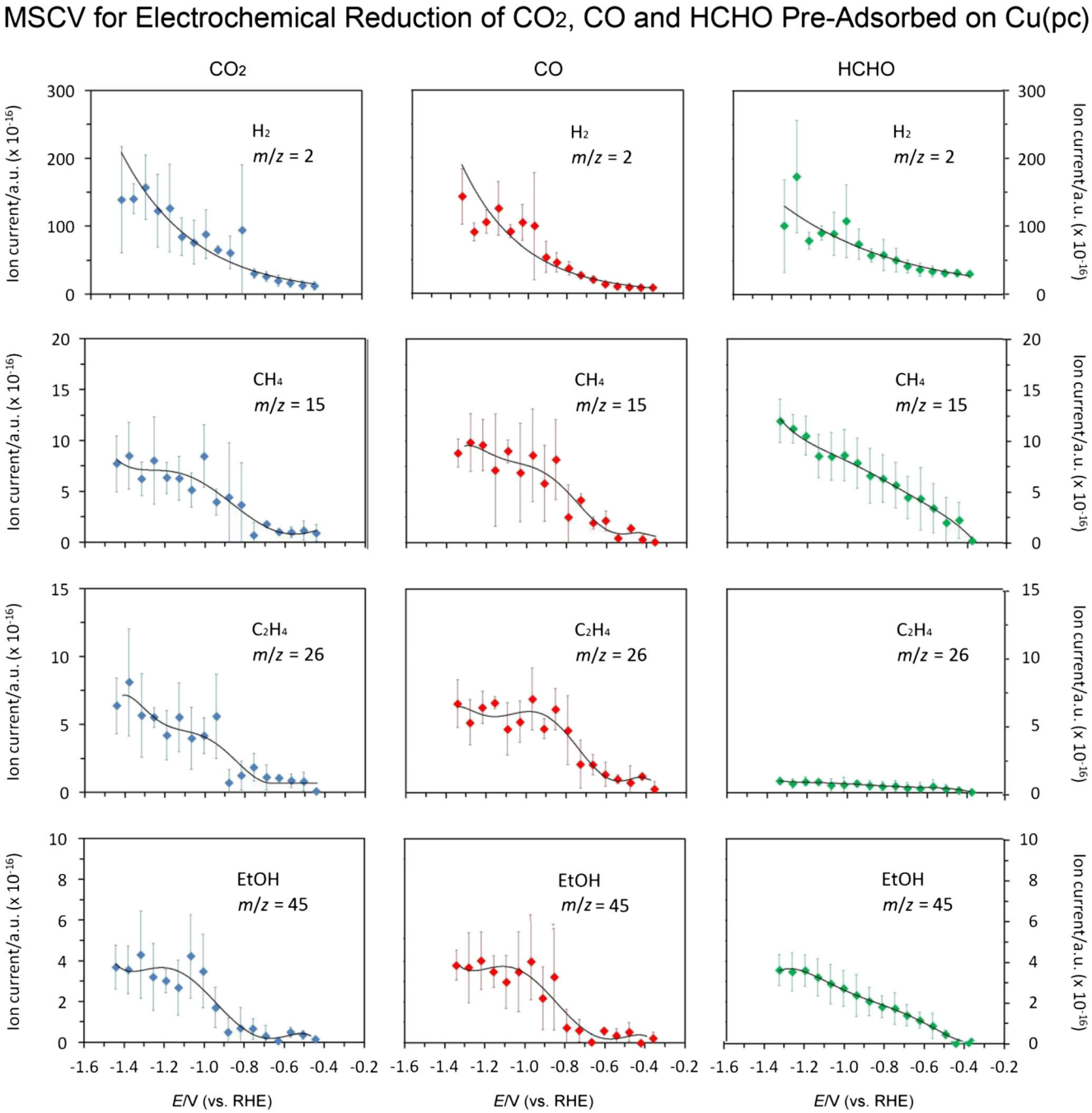

Fig. 2 Mass-spectrometric cyclic voltammograms (MSCV) obtained simultaneously with the current-potential plots in Fig. 1. The response time for the CV curves (Fig. 1) is ca. 1 s faster than that for the MSCV plots; that is, there is a 1 mV difference in the potential axis at a scan rate of 1 mV s^{-1}. The *solid lines* do not represent theoretical simulations but are sextic polynomial fits simply to generate trend lines for easier visual comparisons

times greater than that of CO. (ii) CO is the first product of CO_2 reduction, as well as the first intermediate in more advanced reactions that include formation of pure and oxygenated hydrocarbons; this is in conformity with the (almost) unanimously held view. (iii) HCHO is not a precursor for C=C double-bond formation. (iv) HCHO is an intermediate for the production of methane and ethanol. (v) The generation of CH_4 and CH_3CH_2OH from adsorbed CO occurs via two pathways: one requires a theoretically postulated surface species, protonated CO ($Cu–OCH^+$), and the other involves adsorbed HCHO, constituted after the rate-limiting protonation step. (vi) The generation of CH_4 and CH_3CH_2OH from CO has a substantially higher activation barrier than conversions from HCHO; the latter reactions transpire after the rate-limiting $Cu–OCH^+$ formation and, consequently, are not as highly activated.

Acknowledgments This material is based upon work performed by the Joint Center for Artificial Photosynthesis, a DOE Energy Innovation Hub, supported through the Office of Science of the US Department of Energy under Award No. DE-SC0004993.

References

1. Y. Hori, Mod Asp. Electrochem. **42**, 89 (2008)
2. Y. Hori, H. Wakebe, T. Tsukamoto, O. Koga, Electrochim. Acta **39**, 1833 (1994)
3. K.P. Kuhl, T. Hatsukade, E.R. Cave, D.N. Abram, J. Kibsgaard, T.F. Jaramillo, J. Am. Chem. Soc. **136**, 14107 (2014)
4. K.P. Kuhl, E.R. Cave, D.N. Abram, T.F. Jaramillo, Energy Environ. Sci. **5**, 7050 (2012)
5. M. Gattrell, N. Gupta, A. Co, J. Electroanal. Chem. **594**, 1 (2006)
6. K.J.P. Schouten, Y. Kwon, C.J.M. van der Ham, Z. Qin, M.T.M. Koper, Chem. Sci. **2**, 1902 (2011)
7. C.W. Li, M.W. Kanan, J. Am. Chem. Soc. **134**, 7231 (2012)
8. F. Calle-Vallejo, M.T.M. Koper, Angew. Chem. **125**, 7423 (2013)
9. K.J.P. Schouten, E.P. Gallent, M.T.M. Koper, J. Electroanal. Chem. **716**, 53 (2014)
10. J.H. Baricuatro, C.B. Ehlers, K.D. Cummins, M.P. Soriaga, J.L. Stickney, Y.-G. Kim, J. Electroanal. Chem. **716**, 101 (2014)
11. Y.-G. Kim, M.P. Soriaga, J. Electroanal. Chem. **734**, 7 (2014)
12. Y.-G. Kim, J. H. Baricuatro, A. Javier, J. M. Gregoire, M. P. Soriaga, Langmuir, In press (2014).
13. K.J.P. Schouten, Z. Qin, E.P. Gallent, M.T.M. Koper, J. Am. Chem. Soc. **134**, 9864 (2012)
14. H. Baltruschat, in *Interfacial electrochemistry*, ed. by A. Wieckowski (Marcel Dekker, New York, 1999), p. 577
15. H. Baltruschat, J. Am. Soc. Mass Spectrom. **15**, 1693 (2004)
16. J. Sanabria-Chinchilla, M.P. Soriaga, R. Bussar, H. Baltruschat, J. Appl. Electrochem. **36**, 1253 (2006)
17. J. Sanabria-Chinchilla, J.H. Baricuatro, M.P. Soriaga, F. Hernandez, H. Baltruschat, J. Coll. Interf. Sci. **314**, 152 (2007)
18. J. Sanabria-Chinchilla, Y.-G. Kim, X. Chen, D. Li, H. Baltruschat, M.P. Soriaga, Mod. Asp. Electrochem **44**, 275 (2010)
19. R. Crovetto, J. Phys. Chem. Ref. Data **20**, 575 (1991)
20. S. Vollmer, G. Witte, C. Woll, Catal. Lett. **77**, 97 (2001)
21. R.A. Hadden, H.D. Vandervell, K.C. Waugh, G. Webb, Catal. Lett. **1**, 27 (1988)
22. J.R.B. Gomes, J.A.N.F. Gomes, F. Illas, J. Mol. Catal. A **170**, 187 (2001)
23. A. Forni, G. Wiesenekker, E.J. Baerends, G.F. Tantardini, Int. J. Quantum Chem. **52**, 1067 (1994)
24. A.A. Peterson, F. Abild-Pedersen, F. Studt, J. Rossmeisl, J.K. Norskov, Energy Environ. Sci. **3**, 1311 (2010)
25. A.A. Peterson, J.K. Norskov, J. Phys. Chem. Lett. **3**, 251 (2012)
26. X. Nie, M.R. Esopi, M.J. Janik, A. Asthagiri, Angew. Chem. Int. Ed. **52**, 2459 (2013)